CICERO - A DISTRIBUTED SMALL SATELLITE RADIO OCCULTATION PATHFINDER MISSION

Lee Jasper[1], Danielle Nuding[2], Elliot Barlow[1], Erik Hogan[1], Steven O'Keefe[1]
University of Colorado
[1] ECNT 321, Colorado Center for Astrodynamics, Boulder CO 80309-0431; (303) 492-6734
[2] CIRES 318, Department for Atmospheric and Oceanic Sciences, Boulder CO 80309; (303) 492-1433
Lee.Jasper@Colorado.edu

Pete Withnell
Laboratory for Atmospheric and Space Physics
LSTB-A246, 1234 Innovation Drive, Boulder, CO 80303; (303) 492-1326
Pete.Withnell@lasp.colorado.edu

Thomas Yunck
GeoOptics Inc.
GeoOptics, Inc. 201 N Orange Grove Suite 503, Pasadena, CA 91103; (713)296-0293
tom@geooptics.com

ABSTRACT

Atmospheric limb sounding by GNSS radio occultation has, since the launch of COSMIC, proven to be extremely useful for numerical weather prediction (NWP) climate research and space weather monitoring. Data collection is currently limited by the number of satellites performing GNSS RO measurements, which have so far been the exclusive purview of governmental agencies. The aging of the COSMIC constellation and the fact that currently planned GNSS RO missions will not achieve operational status for several years mean that there is a looming gap in GNSS RO coverage. The Community Initiative for Continuous Earth Remote Observation (CICERO) mission will consist of a network of 24 micro-satellites to expand the current GNSS radio occultation (RO) profile measurements from low Earth orbit (LEO) and fill a data gap caused by expected end-of-life timelines of current RO constellations. The main objective of the CICERO pathfinder mission is to deploy two micro-satellites to demonstrate the capabilities of the CICERO small satellite bus while enhancing weather and climate forecasting capabilities.

INTRODUCTION

Understanding Earth's changing weather and climate is a central goal of atmospheric science, with immense import for society worldwide. GNSS RO profiles provide robust, fundamental measurements of key variables required in climate research and weather forecasting. These data are also of great value in the study of "space weather" – disruptive storms in the ionosphere[1]. GNSS RO has been particularly useful for numerical weather prediction (NWP), providing a significant improvement in global forecasting over the past seven years[2]. The primary measurement made by GNSS RO is atmospheric refractivity, a reflection of temperature, density, pressure, and water vapor content. While such data were obtainable in the past through the use of dropsondes and weather balloons, the advent of GNSS RO provides the added advantages of greater accuracy and comprehensive global coverage[3]. Weather balloons can only provide point source coverage with limited ships for measurements over the ocean. Sounding of the global atmosphere over both land and ocean can be made with high-precision and accuracy using the relatively inexpensive RO technique.

Figure 1: Artist's rendition of CICERO satellite in orbit.

The overall goal of the Community Initiative for Continuous Earth Remote Observation (CICERO) mission is to provide an array of at least 24 (LEO) micro-satellites equipped with specialized, high-performance GNSS receivers. The multi-node approach will provide inexpensive global coverage measurements in contrast to the traditional single sensor approach with

limited coverage. CICERO is slated to fill a gap in data resulting from the expected end of life of current RO satellite missions.

Radio occultation limb-sounding techniques have been demonstrated by several small payload missions, notably COSMIC, SAC-C, and CHAMP. With a relatively inexpensive GNSS receiver, the phase delay of radio waves from existing GNSS satellites can be measured as they are occulted by Earth's atmosphere. The refractive angles of radio wave trajectories can provide accurate vertical profiles of the troposphere, stratosphere, and ionosphere[1]. Refractivity profiles can be used to derive temperature, pressure, and water vapor concentrations, refractive index values, and electron densities through a variety of inversion techniques. These variables are of fundamental importance in operational numerical weather prediction, climate, and space weather monitoring.

The CICERO pathfinder spacecraft, are being designed, built, and operated by the Laboratory for Atmospheric and Space Physics (LASP) in conjunction with GeoOptics Inc. The CICERO pathfinder mission consists of two identical micro-satellites and will provide global RO profiles to enhance the terrestrial atmospheric dataset made available to scientists and decision makers worldwide. CICERO's custom structural design provides optimum antenna placement for GNSS RO measurements while still accommodating the spacecraft bus requirements. The attitude determination and control system (ADCS) utilizes a traditional set of hardware for three-axis stabilization, and a control estimation algorithm based on modified Rodrigues parameters rather than quarternions to define rotations in three dimensions. Through the use of COTS hardware and a modified class B EEE parts program, the CICERO pathfinder spacecraft can be quickly and inexpensively deployed.

RADIO OCCULTATION AND WEATHER PREDICTION

GNSS radio occultations occur when a satellite orbiting in LEO observes GNSS transmissions emanating from a satellite appearing to set behind the limb of the Earth, recording the GNSS transmissions as they pass through the ionosphere and atmosphere. From LEO, there are typically 12 or more GPS satellites visible at any one time, plus additional satellites of the Russian GLONASS satellite navigation system, with a high likelihood of multiple satellites passing through the field of view of the LEO satellite's antennas. The geometry is driven by motion of the LEO, with occultations occurring in the ram (rising) and anti-ram (setting) directions, near the velocity vector direction. This geometry is completely deterministic and can be readily predicted using orbital mechanics, given the LEO and GNSS orbital ephemerides. During an occultation event (typically ~100 seconds), GNSS carrier phase and Doppler are the key observables. Measurement rates can be up to 1 kHz, but can be as low as 1 Hz for ionospheric measurements. Once the Level 0 data is received at the science data processing center, Level 1 products can be retrieved for density, refractivity, temperature, pressure, and water vapor profiles for the troposphere, stratosphere, and ionosphere. Any given atmospheric profile is the retrieval product plotted as a function of height and is derived from an occultation event by use of an inverse Abel transform and other retrieval steps. The horizontal and vertical resolution is dependent on the density of the atmospheric region and higher resolution for regions with higher densities can be expected.

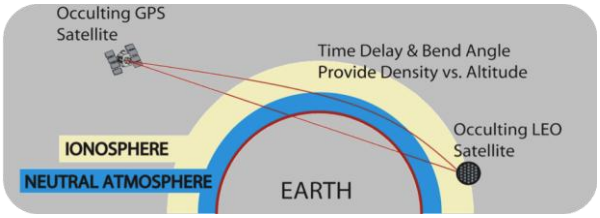

Figure 2: Schematic representation of GPS occultation profile measurement technique. Occulting LEO satellite tracks two signals from GPS satellite as it passes through the ionosphere and neutral atmosphere. The characteristic time delay and bending profile provides raw data necessary for atmospheric and ionospheric profiles of bending angle and refractivity. Image credit: UCAR/COSMIC

In order to perform an accurate retrieval, precise orbit determination of the LEO spacecraft is required. Dual frequency phase observables (using some combination of L1, L2, and L5 signals) are also required to correct for ionospheric delays in retrievals, and are used to perform accurate and precise measurements of ionospheric density. The LEO spacecraft must track at least six non-occulting GNSS satellites to achieve the necessary precision in the orbit estimates for ground processing of the raw data products. POD solutions need only be generated at a rate of 1 Hz and interpolated as necessary, while science measurements will be collected at a rate of 50 Hz. In addition to the occulting satellite, pseudorange and phase measurements from another satellite at higher elevation are used as a reference in a single-differencing method in order to cancel out the effects of the receiver clock. Measurement errors are dominated by the

receiver noise figure at the first amplifier, multipath (reflections of the signal) from spacecraft surfaces near the antennas, and the precision of the knowledge of the spacecraft antenna location. Noise errors can be mitigated by increasing the RO antenna gain, implementing a low noise amplifier, and carefully eliminating contributions of RF interference from the spacecraft. Multipath errors can be mitigated by using a large antenna ground plane though structural design, and using a wideband processing receiver.

Table 1 provides the basic science requirements for the CICERO pathfinder satellites.

Table 1: Mission Measurement Requirements

Data	Threshold
Number of Profiles	565
Neutral Atmosphere Range (km)	2 – 60
Resolution: 0 - 25 km	0.1
Resolution: 25 - 60 km	1.0
Ionosphere Range (km)	60 - 500
Resolution: 60 - 100 km	1
Resolution: 100 - 500 km	2
Average Latency (min)	90

CICERO DESIGN

The CICERO satellite design team consists of engineering professionals, undergraduate and graduate students from electrical, aerospace, and mechanical engineering, as well as atmospheric science departments. The diverse makeup of the design team enables engineering students to gain valuable hands-on design experience creating a knowledgeable and experienced set of early career professionals in the engineering community.

CICERO Mission Parameters

The CICERO Pathfinder Mission will be a secondary payload operating on a near-circular, polar, sun-synchronous orbit. With no critical consumables or single-string limited life items, the nominal lifetime is expected to be at least five years. While in orbit, the CICERO spacecraft will perform RO measurements and transmit the data through a ground station network to the science operations center for processing and distribution with an average latency of 90 minutes from on-orbit data acquisition.

Table 2: Orbital Parameters

Parameters	
Altitude	650 km (±50 km)
Eccentricity	0 (circular)
Inclination	98 deg, 1:30 am
Spacecraft separation	50 deg. true anomaly

The altitude and eccentricity were chosen so as to maximize the number, and optimize the distribution of atmospheric soundings. The mission lifetime will allow for full demonstration of the platform's capabilities while helping to fill the data gap during the development of the remainder of the constellation.

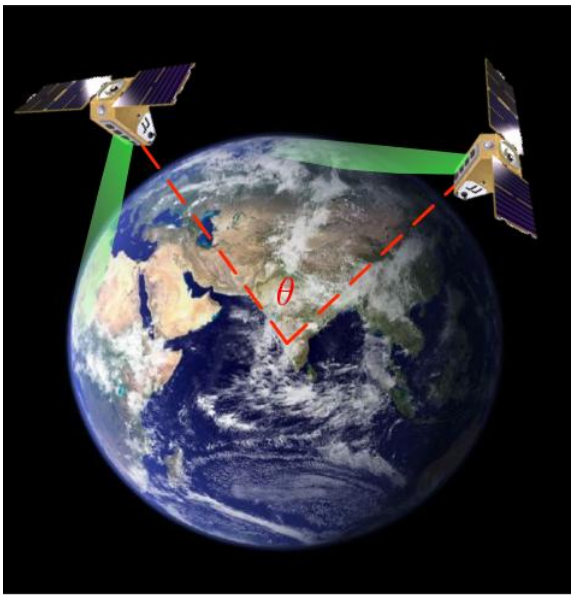

Figure 3 CICERO pathfinder satellites scanning different sections of the atmosphere. $\theta \geq 50°$

The CICERO pathfinder satellites will be launched on the same launch vehicle. To maximize the science return, each satellite carries a cold gas propulsion system used to separate the satellites. The initial close phasing of the satellites allows for overlapping simultaneous measurements. This period will help complete the calibration on the GNSS subsystem to assure measurement accuracy once the two satellites are in their final separated positions. The two spacecraft need to be separated by over 50° of true anomaly in their orbits in their final configuration, shown in Figure 3. The separation allows for unique segments of the atmosphere to be observed by each spacecraft concurrently, increasing the overall data coverage range.

Spacecraft Design

The micro-satellite's exterior has been structurally designed to accommodate two arrays of four RO patch antennas and two hemispherical antennas for precise orbit determination (POD) antennas (Figure 4). The RO antennas are strategically placed on the ram and anti-ram panels to point the peak gain at the limb of the Earth to improve the resolution of the lower troposphere measurements by maximizing the received SNR. The lower troposphere is a key region of interest for weather forecasters. Two POD antennas are pointed slightly above the ram and anti-ram directions to increase the number of ionospheric profiles and to provide position, velocity, and time data for all science measurements. The orientation of the POD antennas enhances the ionosphere science return by increasing the number of occultations in the field of view and providing overlap with the RO antennas in the upper atmosphere.

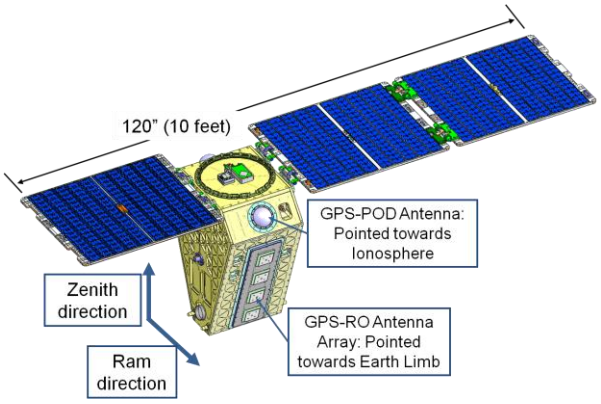

Figure 4: The CICERO Spacecraft

The spacecraft shape also creates an excellent FOV for the communications antennas and coarse sun sensors (CSS) which are on the zenith and nadir facing panels of the spacecraft in Figure 4.

The bus is capable of providing over 100 W of power, up to 10 Mbps data rates to the ground with an expected data volume of 35 MB per orbit, and a sub-arc*min three-axis stabilization platform for RO antenna pointing with a total spacecraft mass of 100 kg.

GNSS Subsystem

The GNSS subsystem is considered to be inclusive of the receiver ("the instrument"), the antennas (both RO and POD), and the front-end components and cabling. Similar to other GNSS RO missions that have already flown, CICERO requires careful selection of components for the front-end, specifically a band-pass filter with a low noise figure across the L-band, and a low-noise amplifier with low noise and high gain. The SNR loss from the cabling has been limited to less than 0.4 dB by careful cable selection and routing.

The GNSS receiver is designed for use in space for GNSS science purposes, specifically RO and reflections. An advantage of GNSS RO is that one subsystem can combine the functions of orbit determination and science data gathering, reducing the overall mass and power requirements of the satellite. RO measurements will be made using a single-differencing technique, so the receiver does not require an ultra-stable oscillator. Occultation scheduling will be performed autonomously by the receiver, and raw observables collected at 50 Hz will be downlinked to for processing into atmospheric profiles on the ground.

The CICERO RO antennas are required to maximize the gain in the direction of the Earth's limb, and also to make stable phase measurements with a minimum of noise. GNSS signals passing through the low atmosphere experience a great deal of atmospheric fading and noise. Focusing the directivity of the antenna in a narrow elevation band pointed at the Earth's limb pushes the lower altitude range of retrieved profiles down while also increasing the number of available occultation opportunities.

Controlling the systematic errors and measurement quality from the antenna is accomplished by limiting the maximum allowable antenna phase gradients present in the phase pattern. If, during an occultation, the ray path of the incoming signal traverses such a gradient it will be observed by the receiver as an unmodelled change in phase; a phase error. During normal operations, there are two causes of ray path motion over the antenna pattern. Observing a satellite as it appears to rise or set behind the limb of the Earth entails a change in the incoming ray's elevation angle averaging approximately three degrees. Secondly, the spacecraft maintains a nadir-pointing attitude, requiring a small, though essentially constant rotation. Because the requirement on the antenna phase gradient trades with the attitude motion requirement, a value of one degree of GPS L1 phase per one degree of phase pattern was chosen for the antenna in order to retain margin in the attitude motion requirements.

ADCS CAPABILITIES

In order to achieve the CICERO science requirements, the spacecraft must point within 1° of nadir, and point the RO antennas within 1° of ram/anti-ram with no more than .15°/s of angular velocity in any axis. Further, the knowledge of the attitude must be within

.1° and the knowledge of the angular velocity must be 0.05°/s.

These requirements are achieved using a three-axis stabilized ADCS system. The system utilizes conventional components for determination such as a star tracker (ST), an inertial measurement unit (rate gyro), and the GNSS receiver. For controlling the spacecraft, a pyramid of four reaction wheels (RWs) is used along with magnetic torque bars (MTBs) and a magnetometer that help to continuously desaturate the wheels.

CICERO operates in two primary attitude states: nadir-pointing and sun-pointing. Sun-pointing state achieves a safe power-positive attitude by pointing the solar panels towards the sun. The satellite utilizes coarse sun sensors (CSS) to achieve this attitude. While these sun sensors are not used for overly accurate pointing, their design and data output achieve pointing within several degrees of the sun vector. This is exciting because the CSS is fairly inexpensive and performs very well with the estimation algorithms used (see the Attitude Determination and Estimation section). Nadir-pointing state requires the use of GNSS receiver POD data and the star tracker. The overall pointing requirements for nadir mode are moderately stringent (1° and .1° knowledge); however, the ADCS system is quite capable of providing this level of precision. Additionally, this pointing can be provided for an indefinite amount of time due to the continuous momentum dumping provided by the MTBs. The control system itself is driven by a unique, globally stable nonlinear feedback law.

The third ADCS state, the thrusting state, is used to control the satellite during propulsion burns. Because the pathfinder mission comprises two satellites that will take separate measurements of the atmosphere, the satellites must have an anomaly separation of 50°. In order to achieve this separation using a single launch vehicle, a propulsion system is required. The thruster is very low force but requires the ADCS to achieve and maintain pointing of the nozzle within 1°-3° aligned with ram/anti-ram during thrusting in order to attain the desired orbit change. Therefore, the CICERO pathfinder satellite is capable of maintaining attitude during orbit maneuvering and station keeping events.

The following sections present several unique components of the CICERO ADCS system. The estimator routines are briefly explained and their capabilities are shown. Then, the control law is explored and simulation results are shown.

Attitude Determination and Estimation

The estimation and control algorithms are defined in terms of the Modified Rodriguez Parameters (MRPs) which are computationally efficient attitude parameters [4]. However, MRPs are minimal and therefore become singular, in this case at 180° rotations. MRPs are also non-unique, a fact which makes it possible to avoid these singularities by simply using what is known as the 'shadow set'. For greater detail on MRPs, see [6].

There are two primary attitude determination algorithms, one for sun-pointing and the other for nadir-pointing. At the moment of separation from the launch vehicle, the spacecraft must achieve sun-pointing within a few orbits to ensure that the batteries are not drained. The attitude determination system is fully capable of estimating the sun's direction with data from the CSS, while using the rate gyro data to detumble the spacecraft.

The sun-pointing state used by CICERO provides the initial start-up conditions of the spacecraft and is reverted to during any safe mode events. Sun-pointing state is a reduced power state and requires a simple, reliable sensor to determine the sun's direction: the CSS.

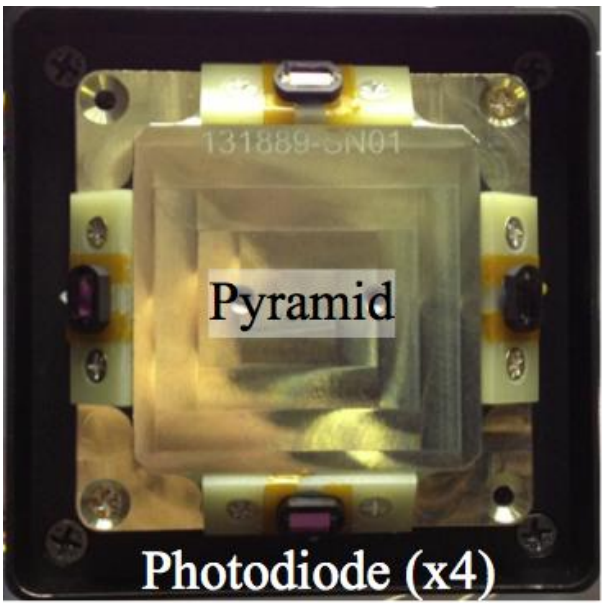

Figure 5: CSS Pyramid with 4 diodes covering half a hemisphere

Figure 5 shows the CSS pyramid with four diodes that can fully observe a half hemisphere about the spacecraft. There are two CSS, one on the zenith panel and one on the nadir panel of the spacecraft. This allows for the sun to be found in any orientation of the

spacecraft, as demonstrated by the ideal FOV plot in Figure 6.

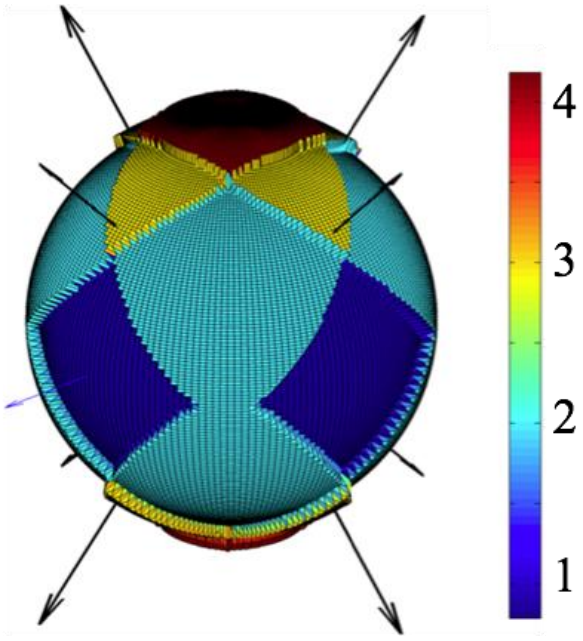

Figure 6: Number of diodes 'seeing' sun, covering entire sphere. Arrows are diode normal vectors

Figure 6 and the estimation algorithms are based upon the idea that each diode produces a set voltage for a given sun incident angle on the diode surface. This angle, given by β in Figure 7 produces a cone on which the sun vector can lie. The spacecraft will begin pointing the spacecraft towards the direction that is observed by the CSS. As more sensors see the sun, the intersection between these cones produces more exact positioning of the sun vector. Three or more sensors observing the sun at the same time are needed to uniquely determine the sun's direction.

$$\hat{n} = \begin{bmatrix} 1 & 0 & 0 \end{bmatrix}$$

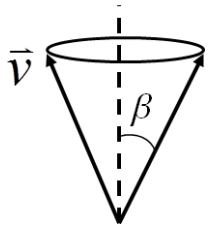

Figure 7: Diode FOV. The normal ($\hat{n}$) from the diode surface is shown along with the sun direction $\vec{v}$

The filters model the angle using a dot product as shown in Eq. 1.

$$\cos(\beta) = \frac{\hat{n} \bullet \vec{v}}{|\vec{v}|} \tag{1}$$

There are two primary filters considered. One uses a weighted estimate of the sun vector through the equation

$$\hat{\vec{v}} = \frac{\sum_{i=1}^{N} \beta_i \hat{n}_i}{\left\| \sum_{i=1}^{N} \beta_i \hat{n}_i \right\|} \tag{2}$$

where N is the total number of sensors. A Kalman filter is utilized assuming the absolute maximum values of the CSS output are known. The Kalman filter operates under the assumption that the sun vector is not changing significantly during the measurement time frame, and the only observed change is due to the spacecraft rotation. This assumption leads to Eq. 3. For greater detail, see [5].

$$\dot{\hat{\vec{v}}} = \vec{\omega} \times \hat{\vec{v}} \tag{3}$$

Placing the diode data into the dynamics and control model for CICERO, the behavior of sun-pointing state is quantified. The simulation scenario uses the orbital parameters from Table 2 and initially assumes the spacecraft has been kicked-off from the launch vehicle with a 2°/s rotation rate on all axes. As a result, the attitude determination system needs to find the sun from a 'lost-in-space' perspective.

The simulation calculates 1.5 orbits and in this case, two diodes are initially seeing the sun, as seen in Figure 8. Using Eq. 3 and estimating the possible positions of the sun due to the two measurements, the spacecraft begins reorienting itself. In a short period of time, sensors three and four are in the sunlight. With four sensors seeing the sun, the zenith panel is completely illuminated, meaning the spacecraft has properly oriented the spacecraft to sun-pointing state. Figure 9 shows the angle between the sun and the solar panels.

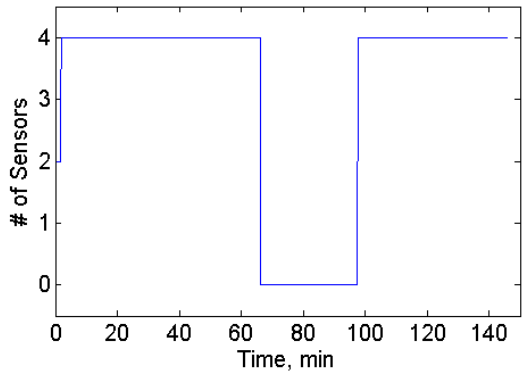

Figure 8: Number of diodes seeing the sun

Sun-pointing state is defined as pointing the solar panels to within 30 degrees of the sun (achieving power-positive conditions). The simulations show that this requirement is met in one minute. Over a range of Monte Carlo runs, it usually takes less than five minutes to achieve sun pointing. This demonstrates that the CSS and estimation system perform very quickly with a simple system.

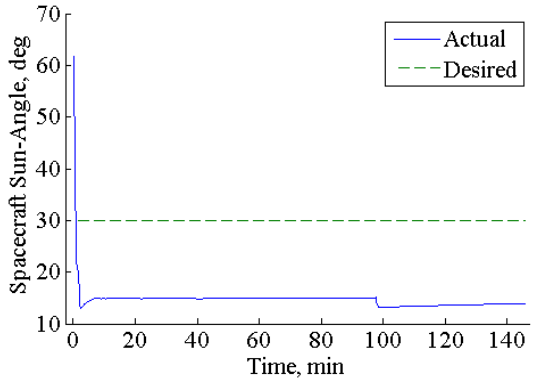

Figure 9: Angle between solar panel normal and sun vector (requirement < 30°)

Figure 8 indicates the sun sensors stop seeing the sun at 60 minutes; this is due to solar eclipse. Note that at the same in Figure 9, the spacecraft sun-angle does not significantly change. During solar eclipse, the on-board system maintains the same orientation. When the satellite emerges from Earth's shadow (at about 100 min), the solar panels generally remain pointed toward the sun. The pointing angle is slightly adjusted by the ADCS system but the satellite maintains the correct orientation during solar eclipse.

For the nadir-pointing estimation, the GNSS system provides position, while the star tracker provides high accuracy attitude knowledge. This coupled with a rate gyro allows the spacecraft to maintain nadir-pointing state. [4] discusses the detailed methodology for determining the state of the spacecraft. Briefly, by using a computationally efficient method, the Kalman filter with MRPs generates an estimate of the spacecraft state, including the rate gyro bias. This approach provides system capability of sub-degree attitude knowledge.

Globally Stabilizing Attitude Control

The control developed for the CICERO mission is very capable, allowing for three-axis control and 1° pointing with angular rates of less than 0.05°/s.

The controller is based upon a Lyapunov, globally stable control law development:

$$V = \frac{1}{2}\delta\bar{\omega}^T[I]\delta\bar{\omega} + 2K\ln(1+\bar{\sigma}^T\bar{\sigma}) + \frac{1}{2}\bar{z}^T[K_I]\bar{z} \qquad (4)$$

where $\delta\bar{\omega} = \bar{\omega} - \bar{\omega}_R$ is the body rates minus the desired reference rates, K is a scalar gain, σ are the MRPs, $[K_I]$ is a gain matrix and z is the integral term:

$$\bar{z} = \int_0^t (K\bar{\sigma} + [I]\delta\dot{\bar{\omega}})dt \qquad (5)$$

Because this control law is globally stable, it can handle *all* desired attitude states. Therefore, detumbling, sun-pointing, nadir-pointing and thrusting states can all be achieved with this single law. This simplifies the development and testing time required to verify the ADCS system due to the fact that there are not multiple controls that need to be verified. Note that the control's derivation is shown in more detail in[7].

The control algorithms are also enhanced through continuous momentum dumping for the reaction wheels, so that they do not saturate (i.e. reach maximum wheel speeds). Continuous momentum dumping can be created due to the null space available to the spacecraft control system from having seven actuators (four RW and three MTBs) for a three degree of freedom system. The desired control torque for the wheels is computed from the Lyapunov control that is derived from Eq. 4. Again, the detailed development is given in [7]. The basic premise can be outlined by Eq. 6:

$$\bar{\tau}_T = \Delta\bar{\tau} + \bar{\tau}_{desaturate} + \bar{\tau}_{desired} \qquad (6)$$

In this equation $\bar{\tau}_{desired}$ is the desired, computed torque from the control law, $\bar{\tau}_{desaturate}$ is the torque required to despin each wheel to a desired spin rate, and $\Delta\bar{\tau}$ represents the difference between the capability of the

torque bars and the desaturation torque. The summation of these allow for proper desaturation of the wheels.

The orbital parameters from Table 2 are used are used to run a simulation to demonstrate the control system with an initial kick-off rotation rate of 2°/s on all axes. The simulation demonstrates acquisition of a sun-pointing attitude, after solar panel deployment, for 250 minutes at which point it transitions into nadir-pointing state. Figure 10 shows the principal rotation angle error between the body and the reference trajectory. The body quickly achieves sun-pointing and the error approaches zero, therefore there is no error shown on the log scale between 0 and 250 minutes. Figure 11 demonstrates the exchange of angular momentum from the spacecraft to the wheels as the wheels spin-up. The wheel rates reduce and achieve the desired offsets around 250 rpm due to the momentum dumping provided by the torque bars. At 250 minutes, the wheels again increase in rpm to maneuver the spacecraft to a nadir-pointing attitude. Momentum dumping occurs throughout the remainder of the simulation. The wheel rates, however, never achieve the desired wheel offsets due to the constant application of torque to account for constantly changing attitude in nadir-pointing state. Note that the wheels do keep a relatively bounded speed profile, indicating that the momentum dumping continues to function. Figure 11 shows that sub-degree pointing is achieved for the nadir-pointing state, meeting requirements.

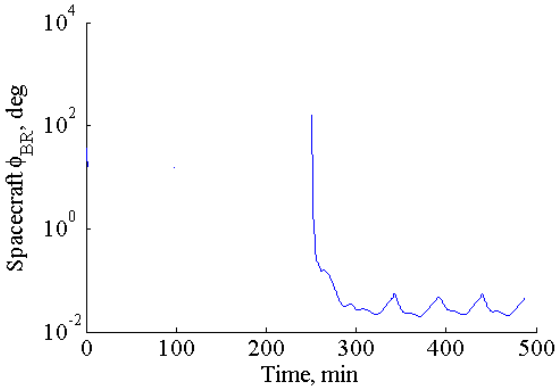

Figure 10: Principal rotation angle between reference (desired) attitude and body attitude

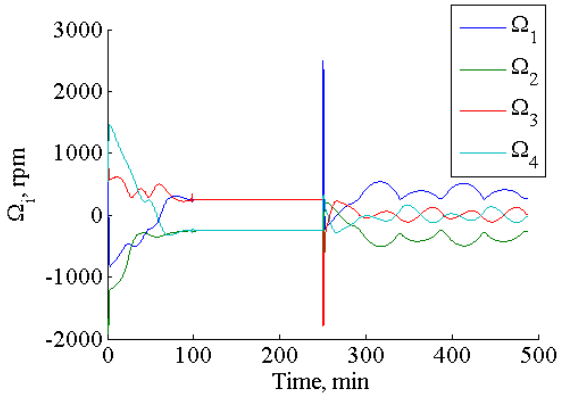

Figure 11: Reaction wheel speeds from kick-off to sun-pointing state. Nadir-pointing state engaged at 250 minutes

CONCLUSIONS

GNSS radio occultation measurements are now being used by several major weather prediction centers worldwide, including NOAA[8], and the ECMWF[9]. GNSS RO requires only a GNSS receiver in orbit, already a mature technology, and can generate atmospheric profiles just as easily over the ocean as over land. The advantages provided by GNSS RO over traditional data-gathering methods like radiosondes, specifically the global distribution, measurement precision, and low marginal cost, ensure that their use will only continue to increase with time. At the same time, the existing and planned governmental RO constellations schedule will leave a significant multi-year gap in GNSS RO coverage. In addition to depriving NWP centers of valuable data, a gap such as this is detrimental to climatology studies as the overlap between separate data sources provides an important calibration.

CICERO has been designed expressly to meet the need for GNSS RO with low-cost COTS parts and short development time without sacrificing measurement quality. With the exception of the GNSS receiver and antenna, emphasis has been placed on using COTS equipment for all subsystems along with a class B EEE parts program to facilitate the usage of commercial parts that have not yet been flight-approved when required and possible at the discretion of the experts. The GNSS receiver itself will use existing technology and only the RO antenna requires a novel, specialized design. The ADCS system utilizes a number of novel features adapted to COTS hardware, achieving very high levels of precision and accuracy. Finally, CICERO manages to achieve all of its mission requirements using a rather small (~1 m longest dimension) and simple but robust spacecraft bus. This pathfinder mission will provide valuable insights and

lessons learned for the full constellation, scheduled to follow within two years.

Given the current need for GNSS RO data at low cost, CICERO is ideal fit. By using relatively inexpensive hardware for the spacecraft bus, CICERO will be able to provide RO data products at a fraction of the cost required for existing RO constellations. CICERO's development also integrates a team of seasoned technical professionals with students, seeding the next generation of engineers and specialists.

Acknowledgments

The authors would like to acknowledge the Laboratory for Atmospheric and Space Physics, GeoOptics Inc., and the CICERO team for their support and dedication to the CICERO project. They would also like to acknowledge Dr. Hanspeter Schaub for his work on the attitude determination and control system, John Kreicher for his excellent design of the coarse sun sensor, and Dr. Penina Axelrad for her efforts on the RO instrument.

References

1. Kursinski, E. R., G. A. Hajj, J. T. Schofield, R. P. Linfield, and K. R. Hardy. "Observing Earth's Atmosphere with Radio Occultation Measurements Using the Global Positioning System." *Journal of Geophysical Research* 102.D19 (1997): 23429-3465.
2. Collard, A. D., and S. B. Healy. "The Combined Impact of Future Space-based Atmospheric Sounding Instruments on Numerical Weather-prediction Analysis Fields: A Simulation Study." *Quarterly Journal of the Royal Meteorological Society* 129.593 (2003): 2741-760.
3. Kuo, Y.-H., W. S. Schreiner, J. Wang, D. L. Rossiter, and Y. Zhang. "Comparison of GPS Radio Occultation Soundings with Radiosondes." *Geophysical Research Letters* 32.5 (2005)
4. O'Keefe, S. and Schaub, H, "Shadow set consideration for modified rodrigues parameter attitude filtering", AAS/AIAA Astrodynamics Specialist Conference, Hilton Head, SC, August 2013.
5. O'Keefe, S. and Schaub, H, "Sun heading estimation using underdetermined set of coarse sun sensors", AAS/AIAA Astrodynamics Specialist Conference, Hilton Head, SC, August 2013.
6. Schaub, H. and J. L. Junkins, Analytical Mechanics of Space Systems, AIAA Education Series, Reston, VA, 2003.
7. Hogan, E. A. and H. Schaub, "Three-axis Attitude Control Using Redundant Reaction Wheels with Continuous Momentum Dumping," Proceedings of the AAS/AIAA Spaceflight Mechanics Meeting, Kauai, HI, February 2013.
8. Cucurull, L., J. C. Derber, R. Treadon, and R. J. Purser. "Assimilation of Global Positioning System Radio Occultation Observations into NCEP's Global Data Assimilation System." *Monthly Weather Review* 135.9 (2007): 3174-193.
9. Gobiet, A., U. Foelsche, A. L. Steiner, M. Borsche, G. Kirchenghast, and J. Wickert. "Climatological Validation of Stratospheric Temperatures in ECMWF Operational Analyses with CHAMP Radio Occultation Data." *Geophysical Research Letters* 32.12 (2005)